BMC Veterinary Research

RESEARCH

Open Access

Adaptation mechanisms of *Brucella abortus* to low magnesium ion stress

Hengtai Wang[1], Lang Lv[1], Yike Huang[1], Hui Jiang[1], Xiaowen Yang[1], Jiabo Ding[1], Liangquan Zhu[2], Lei Xu[2], Huaiming Sang[3], Jianxia Jiang[3*], Nan Wang[2*] and Peng Li[1*]

Abstract

Background *Brucella abortus*, a facultative intracellular pathogenic bacterium that usually causes diseases under animals and humans, can survive and replicate within phagocytic cells. Within the host cells, *B. abortus* has to adapt to low cytosolic magnesium ion (Mg^{2+}) environment, which is critical for bacterial survival and replication. To understand the fitness of *B. abortus* under the low Mg^{2+} environment, transcriptome analysis was performed by RNA-seq. Results: 262 differentially expressed genes (DEGs, fold-change > 1.5 and $p < 0.05$) of *B. abortus*, 123 significantly upregulated genes and 139 significantly downregulated genes, were identified under Mg^{2+} starvation environment, highlighting that *B. abortus* probably employed large amounts of factors to support the adaptation of low Mg^{2+} stress responses. Amongst them, two key genes, BAB_RS26550 (encoding putative protein, abbreviated as HP3) and BAB_RS26555 (encoding MgtC/SapB family protein, abbreviated as MgtC), was associated with the ATP hydrolysis to maintain the growth and metabolism of *B. abortus* under Mg^{2+} starvation environment. Furthermore, the HP3 supported *B. abortus* to resist bactericidal polycations and polymyxin B, as well as influenced the biofilm formation of *B. abortus*. However, HP3 does not appear to have an appreciable effect on the *B. abortus* virulence. Conclusions: In this study, a first description of the pattern of *B. abortus* genetic expression in response to low Mg^{2+} stress response provides insights into the intracellular behavior of *B. abortus* at the genetic level.

Keywords *Brucella abortus*, Low Mg^{2+}, Transcriptome analysis, MgtC, HP3

Introduction

Brucella abortus, a Gram-negative and facultative intracellular pathogenic bacterium, usually causes brucellosis, a global zoonotic disease characterized by reproductive disease in domestic animals and chronic debilitating disease in humans [1, 2]. The most important feature of *Brucella* virulence is the ability to invade and replicate within professional and non-professional phagocytes, such as macrophages, dendritic cells (DCs), placental trophoblasts and epithelial cells [3]. During the course of infection, *Brucella* will experience different stress environments, such as acid conditions, nutrient limitation, and then modulate their gene expression assisting *Brucella* to survive and replicate within host cells [4]. Within

*Correspondence:
Jianxia Jiang
jjxcasey@njmu.edu.cn
Nan Wang
15120089648@163.com
Peng Li
lipeng01@caas.cn
[1]Key Laboratory of Animal Biosafety Risk Prevention and Control (North) of MARA, Institute of Animal Science, Chinese Academy of Agricultural Sciences, Beijing 100193, China
[2]National/WOAH Reference Laboratory for Brucellosis, FAO Reference Centre for Brucellosis, China Institute of Veterinary Drug Control, Beijing 100193, China
[3]Department of Gastroenterology, The First Affiliated Hospital of Nanjing Medical University, Nanjing 210029, China

the macrophage phagosome, the intracellular bacterial pathogen also encounters a host-imposed Magnesium ion (Mg^{2+}) limitation [5, 6].

Mg^{2+}, the most abundant multivalent cation in all living cells with a concentration ranging from 5 to 20mM [7], is required for assembly, structure and function of the ribosome [8, 9], stabilization of RNA and DNA [10–12]. Moreover, Mg^{2+} counteracted the negative charges on adenosine triphosphate (ATP) [8], and neutralized the negative charges in outer membrane lipopolysaccharide (LPS) [13]. These results indicated that Mg^{2+} is a key ion for living cells. Furthermore, Mg^{2+} is an extracellular signal that controls the PhoP/PhoQ two-component regulatory system of *Salmonella typhimurium* [14]. Upon the Mg^{2+} starvation environment, the expression of many factors including the Mg^{2+} transporters MgtA and MgtB [15], the enzymes that modify LPS [16], the F_1F_o ATP synthase inhibitory protein MgtC [17] and polyamines [5], were directly activated. *Brucella* strains were predicted to contain Mg^{2+} transport system based on surveys of the publicly available genome sequences, and require Mg^{2+} as an essential micronutrient for optimal growth in vitro [18, 19]. Homologs of two genes associated with Mg^{2+} transport in *Salmonella typhimurium* have been genetically linked to the virulence in *Brucella* strains. One Mg^{2+} transporter, MgtB, was involved in *Brucella melitensis* pathogenesis in experimentally infected mice [20]. In *Salmonella*, MgtC inhibits the activity of the F_1F_o ATP synthase by direct interaction, hindering ATP-driven proton translocation and NADH-driven ATP synthesis in inverted vesicles [17]. *Brucella suis* MgtC was associated with its growth in a Mg^{2+}-restricted medium and its virulence in the murine macrophage-like J774 cell line [21]. *B. abortus* employed MgtC to maintain its metabolism through supporting the ATP hydrolysis in low Mg^{2+} environment [26]. However, the research about adaptation of *B. abortus* under the low Mg^{2+} stress response is missing. Therefore, it is of interest to identify the resistance determinants responsible for the adaptation of *B. abortus* to low Mg^{2+} stress responses.

A description of the pattern of genetic expression in response to low Mg^{2+} stress response would possibly provide insights into the intracellular behavior of *Brucella* at the genetic level. In the present study, we reported that five continuous genes upregulated in *B. abortus* under low Mg^{2+} conditions were identified by RNA-seq. Among them, two genes, hypothetical protein gene (BAB_RS26550) and *mgtC* (BAB_RS26555), were associated with the bacterial growth under low Mg^{2+} conditions by influencing bacterial ATP concentrations. The obtained results provide relevant information in the adaptation of *B. abortus* to low Mg^{2+} stress responses.

Materials and methods

Strains, plasmids, macrophages, and culture conditions

All strains and plasmids used in this study are listed in Table 1. *B. abortus* 2308 from the National Center for Veterinary Culture Collection (CVCC, China) and its derivatives were cultured in tryptic soy broth (TSB) or on tryptic soy agar (TSA) (Difco, Franklin Lakes, NJ, USA) at a temperature of 37 °C with 5% CO_2 in a BSL3 biosafety laboratory. *E. coli* DH5α employed in recombination and transduction experiments were cultivated in Luria-Bertani (LB) medium at a temperature of 37 ℃. When necessary, the culture medium was supplemented with 100 μg/mL ampicillin and 25 μg/mL of chloramphenicol. *B. abortus* 2308 and its derivatives were grown in M9 medium supplemented with 0.1% casamino acids, 1% yeast extract, 1% arabinose and 10 μM $MgCl_2$ (low Mg^{2+} conditions) or in M9 medium supplemented with 0.1% casamino acids, 1% yeast extract, 1% arabinose and 10 mM $MgCl_2$ (high Mg^{2+} conditions). RAW264.7 cells (ATCC, Manassas, VA, USA) were cultured at a temperature of 37 °C with 5% CO_2, using Dulbecco's modified Eagle's medium (DMEM) supplemented with either 10% or 1% heat-inactivated fetal bovine serum (Gibco, Thermo Scientific Grand Island, NY, USA).

Plasmids and mutant construction

Primers for construction were designed using the sequence of the target genes *HP1*, *MgtA*, *HP2*, *HP3*, *MgtC* or *HP1-MgtC* in the *B. abortus* S2308 genome (GenBank Code: NC_007618.1). All primers used in this study are listed in Table S1. The mutant strain was constructed according to the previously published protocol [22]. Suicide plasmids were constructed, using an overlap PCR assay. Briefly, the upstream and downstream fragments of the target genes *HP1*, *MgtA*, *HP2*, *HP3*, *MgtC* or *HP1-MgtC* were amplified in two independent PCR reactions using PrimeSTAR Max Mix (TaKaRa, Dalian, China) with primer pairs, and then recovered PCR products were used as templates for overlap PCR to produce joint sequences with primer pairs. The product of overlap PCR that contained joined flanking sequences was purified by gel extraction, digested with *Xba*I and *Sac*I, and ligated into a pUC19-*sacB* plasmid to generate the suicide plasmids. The suicide plasmids were propagated in *E. coli* DH5α cells (Invitrogen Corp., Carlsbad, CA, USA) and then extracted to construct the mutant strains. These vectors were sequenced to confirm its accuracy. Allelic replacement was employed to delete the target genes *HP1*, *MgtA*, *HP2*, *HP3*, *MgtC* or *HP1-MgtC* from the wild-type strain S2308. S2308 was cultured and collected by centrifugation at the exponential phase. After an ice bath for 15 min, S2308 was washed twice with ice-cold sterile water. Bacteria were resuspended in 10% (v/v) glycerin water and 3–5 μg suicide plasmid was added on

Table 1 Strains and plasmids used in the present study

Names	Description	Source
Strains		
B. abortus	Wild-type strain 2308	CVCC
S2308Δ*HP1*	*HP1* deleted mutant	This study
S2308Δ*MgtA*	*MgtA* deleted mutant	This study
S2308Δ*HP2*	*HP2* deleted mutant	This study
S2308Δ*HP3*	*HP3* deleted mutant	This study
S2308Δ*MgtC*	*MgtC* deleted mutant	This study
S2308Δ*HP1-MgtC*	*HP1*, *MgtA*, *HP2*, *HP3*, *MgtC* deleted mutant	This study
E. coli DH5α	F – φ80lacZΔM15Δ(lacZYA-argF)U169 recA1 endA1 hsdR17(rk–,mk+) phoA supE44 thi-1 gyrA96 relA1 λ–	Invitrogen
Plasmids		
pUC19-*sacB*	Amp^R; pUC19 derived plasmid containing *sacB* gene	[43]
pUC19-*sacB*-Δ*HP1*	Amp^R; pUC19-*sacB* containing the upstream and downstream fragments of the *HP1* gene	This study
pUC19-*sacB* -Δ*MgtA*	Amp^R; pUC19-*sacB* containing the upstream and downstream fragments of the *MgtA* gene	This study
pUC19-*sacB* -Δ*HP2*	Amp^R; pUC19-*sacB* containing the upstream and downstream fragments of the *HP2* gene	This study
pUC19-*sacB* -Δ*HP3*	Amp^R; pUC19-*sacB* containing the upstream and downstream fragments of the *HP3* gene	This study
pUC19-*sacB* -Δ*MgtC*	Amp^R; pUC19-*sacB* containing the upstream and downstream fragments of the *MgtC* gene	This study
pUC19-*sacB*-Δ*HP1-MgtC*	Amp^R; pUC19-*sacB* containing the upstream and downstream fragments of the five consecutive genes *HP*, *MgtA*, *HP2*, *HP3*, *MgtC* gene	This study
pBBR1MCS1	Cm^r; Broad-host-range cloning vector; parental plasmid	[44]
pBBR1MCS1- *HP1*	Cm^r; pBBR1MCS1 plasmid containing the *HP1* gene	This study
pBBR1MCS1-*MgtA*	Cm^r; pBBR1MCS1 plasmid containing the *MgtA* gene	This study
pBBR1MCS1- *HP2*	Cm^r; pBBR1MCS1plasmid containing the *HP2* gene	This study
pBBR1MCS1- *HP3*	Cm^r; pBBR1MCS1plasmid containing the *HP3* gene	This study
pBBR1MCS1-*MgtC*	Cm^r; pBBR1MCS1 plasmid containing the *MgtC* gene	This study
pBBR1MCS1-*HP1-MgtC*	Cm^r; pBBR1MCS1 plasmid containing the five consecutive genes *HP*, *MgtA*, *HP2*, *HP3*, *MgtC* gene	This study

ice. Then the suicide plasmids were transferred to S2308 by electroporation. After electroporation, transformed S2308 were immediately transferred to prewarmed TSB media and cultured overnight. The first exchanged recombinants were selected by plating on TSA containing ampicillin at 100 μg/mL. The second round of exchanged recombinants was selected by plating on TSA containing 5% sucrose, then the sucrose-resistant colonies were respectively culture on the TSA plate and TSA plate supplemented with 100 μg/mL ampicillin. At least ten colonies that grown on the TSA plate and did not grow on the TSA plate supplemented with 100 μg/mL ampicillin were collected for identification with PCR using outer primer pair of the target genes *HP1*, *MgtA*, *HP2*, *HP3*, *MgtC* or *HP1-MgtC* up-F/down-F, and inner primer pair of the target genes *HP1*, *MgtA*, *HP2*, *HP3*, *MgtC* or *HP1-MgtC* inner-F/inner-R (Table S1). Colonies with length-reduced fragment from up-F/down-F pair and no fragment from inner-F/inner-R were selected as the target genes *HP1*, *MgtA*, *HP2*, *HP3*, *MgtC* or *HP1-MgtC* deleted mutant.

To complement the function of each deleted gene, a complement plasmid was constructed using the broad host-range plasmid pBBR1MCS1. The target gene fragment was amplified by PCR using the primers and gel purified. The recovered fragment was digested with the restriction enzymes *BamH*I and *Hind*III, and then ligated into the *BamH*I- and *Hind*III- digested plasmid pBBR1MCS1. The recombinant complement plasmid was propagated in DH5α cells and extracted to construct the complement strain. These vectors were sequenced to confirm its accuracy. Then the complementary plasmids were transferred to the corresponding mutant by electroporation. The complementary strains were selected by plating on TSA containing chloramphenicol. Analyses of PCRs were carried out to identify clones.

Determination of bacterial growth curves in high or low Mg^{2+} conditions

B. abortus 2308 and its derivatives were cultured in TSB to optical density 600 nm (OD_{600}) at 0.6, and then the bacteria were washed twice with phosphate buffered saline (PBS) (HyClone, GE Lifesciences, Logan, UT, USA) to remove the TSB medium. The bacteria were centrifuged at 8000 × g for 5 min to precipitate bacteria, and the pellets of strains were resuspended in 1mL M9 medium. The cell suspension was serially diluted 10-fold with PBS and spread onto TSA plates to calculate viable bacteria (CFU). To analyze bacterial responses to Mg^{2+}, 1×10^8 CFU of each strain were added to 20 mL M9 medium containing 0.1% casamino acids, 1% yeast extract, 1% arabinose supplemented with 10 μM Mg^{2+} (low Mg^{2+} conditions) or 10 mM Mg^{2+} (high Mg^{2+} conditions). Each strain was incubated at 37 °C with 200 rpm, and OD_{600} of bacteria under different conditions were

measured at the same time points. Bacterial growth curves were recorded by measurement of OD_{600} throughout the incubation period.

RNA extraction and Real-Time PCR

As previously reported [22], total RNA was extracted from bacteria using the RNA simple Total RNA Extraction Kit (TianGen, Beijing, CN) according to the manufacturer's protocol. Genomic DNA contamination was removed through treatment with a ReverTra Ace® qPCR RT Master Mix with gDNA Remover kit (TOYOBO, Shanghai, CN). The RNA quantity and quality were evaluated by calculation of RNA concentration and OD_{260}/OD_{280} ratio using the Thermo Scientific NanoDrop One (Thermo Fisher Scientific, Waltham, MA, USA), and the RNA integrity was assessed by calculation of RNA integrity number using standard denaturing agarose gel electrophoresis. 1 μg RNA was reverse transcribed into cDNA, using a ReverTra Ace® qPCR RT Master Mix with gDNA Remover kit (TOYOBO, Shanghai, CN) according to the manufacturer's instructions. A 20 μL RT-PCR mixture was made comprising 10 μL 2×ChamQ Universal SYBR qPCR Master Mix (Vazyme, NanJing, CN), 1 μL cDNA, 0.5 μL (each) forward and reverse primers (10 μM each), and 8 μL double-distilled water (ddH_2O). The mixture was incubated at 95 °C for 2 min, and then subjected to 40 cycles at 95 °C for 15 s, followed by 60 °C for 1 min using the Applied Biosystems™ 7500 (Thermo Fisher Scientific). All samples were analyzed in triplicate and relative transcription levels of each gene were determined by the $2^{-\Delta\Delta Ct}$ method, using 16 S RNA as an internal control for data normalization. All primers used for RT-PCR are listed in Table S1.

RNA-Seq

Total RNA was extracted from *B. abortus* 2308 cultured under high or low Mg^{2+} minimal medium M9 supplemented with 0.1% casamino acids, 1% yeast extract and 1% arabinose at the mid-phase of cell growth (OD_{600} = 0.6–0.8), respectively, as described above. Subsequently, the cell samples were subjected to RNA-seq global transcriptomic analysis by Shanghai Majorbio Biopharm Technology Co.Ltd, and all samples were analyzed in triplicate. The data were analyzed via the online Majorbio I-Sanger CloudPlatform (https://cloud.majorbio.com). To ensure the quality of sequencing data, SeqPrep (https://github.com/jstjohn/SeqPrep) and Sickle (https://github.com/najoshi/Sickle) with the default settings were used to filter raw data. The genome of *B. abortus* 2308 was used as a reference, and the cleaned reads were aligned to the reference transcriptome using Bowtie 2 (http://bowtie-bio.sourceforge.net/index.shtml). To identify the differentially expressed genes (DEGs) between the samples, gene level transcripts per million reads (TPM) were generated using RSEM Version 1.3.1 (http://deweylab.github.io/RSEM) and DEGs were screened by DESeg2 (http://bioconductor.org/packages/stats/bioc/DESeq2) with FC > 1.5 and p-adjust < 0.05. Then DEGs were further subjected to function annotation and pathway enrichment analysis by hypergeometric distribution testing using Gene Ontology (GO) (http://www.geneontology.org/) and Kyoto Encyclopedia of Genes and Genomes (KEGG) (http://www.genome.jp/kegg/).

Determination of intracellular ATP

ATP concentrations in the bacteria were detected using the ATP content detection kit (Solarbio Lifesciences, Beijing, China) according to the manufacturer's protocol. Briefly, *B. abortus* 2308 and its derivatives were cultured under high or low Mg^{2+} minimal medium M9 supplemented with 0.1% casamino acids, 1% yeast extract and 1% arabinose at the mid-phase of cell growth (OD_{600} = 0.6–0.8), and then the CFU of bacteria were assessed by serially diluting and plate counting. 1×10^7 CFU bacteria were collected by centrifuging at 8,000 × g for 5 min to precipitate bacteria before the experiment. The pellet of bacteria resuspended in the buffer. After treatment, the bacteria were subjected to ultrasonic disruption and 10,000 × g for 10 min at 4 ℃, supernatant was collected for detection. The supernatant was mixed with chlorine and vortexed for 15 to 20 s, followed by centrifuging at 10,000 × g at 4 °C for 3 min. The absorbance of the supernatant at 340 nm was measured.

Stress resistance assays

Stress resistance assays were performed to determine the sensitivity of *B. abortus* 2308 and its derivatives to oxidative stress, cationic bactericidal peptides, acidic stress, Fe^{2+} stress, osmolarity stress, and nitrosative stress, as previously reported [23].

2.5 mM or 5 mM H_2O_2, 200 μg/mL or 500 μg/mL polymyxin B medium, pH 4.5 or 5.5 acid medium were used to determine sensitivity of *B. abortus* 2308 and its derivatives to oxidative stress, cationic bactericidal peptides, and acidic stress. Briefly, *B. abortus* 2308 and its derivatives were cultured to the mid-logarithmic phase (OD_{600} = 0.6–0.8) in TSB, and then the bacteria were diluted with PBS to a concentration of 5×10^8 CFU/mL. 5 μL of bacteria in PBS was mixed with 200 μL of the appropriate medium. After incubation at 37 ℃ with 5% CO_2 for 2 h, the bacterial survival percentages were calculated as: CFU obtained from bacteria treated with different factors / CFU obtained from bacteria in PBS × 100. The calculation is normalized by the volume used in the experiment (CFUs/ml). The results are expressed as the mean percentage of triplicate samples ± standard deviation (SD), and three independent experiments were performed.

4mM 2, 2-bipyridine (Fe^{2+} chelating agent), 200 mM sodium chloride (NaCl), 0.5 mM sodium nitroprusside (SNP) was used to assess sensitivity to Fe^{2+} stress, osmolarity stress, and nitrosative stress. Briefly, *B. abortus* 2308 and its derivatives were cultured to the mid-logarithmic phase in TSB, and then the bacteria were diluted with PBS to a concentration of 5×10^9 CFU/mL. The suspension was serially diluted by 10-fold and 5 µl of the solution was blotted on the TSA containing the appropriate medium and cultured for 3–5 days at 37 °C. TSA without SNP was used as a normal growth control.

Crystal Violet staining

Biofilm formation assay was performed using crystal violet staining according to published protocols [24]. Briefly, overnight cultures of *B. abortus* 2308 and its derivatives were diluted to 1×10^6 CFU/mL in TSB. 200 µL aliquots were transferred into the corresponding wells of 96 well microtiter plate and incubated at 37 °C for 48 h and 96 h. After that, the culture supernatant was discarded and cells were rinsed with PBS. 200 µL crystal violet solution (0.1%, v/v) was added to each well and incubated at 37 °C for 20 min. Subsequently, crystal violet solution was removed, and wells were washed with PBS 4 times in order to remove unattached cells and residual crystal violet. 200 µL of 95% v/v EtOH was added to each well and optical density of released crystal violet was measured at 600 nm.

Bacterial adherence, invasion and cellular survival assay

Bacterial adherence, invasion and intracellular survival were tested using RAW 264.7 cells. Cells were plated in the 24-well plates (Corning, NY, USA) and infected with *B. abortus* S2308 or its derivatives at a multiplicity of infection (MOI) of 100 CFU per cell. To synchronize the infection, the infected plates were centrifuged at 400 × g for 5 min, and cells were then incubated at 37 °C with 5% CO_2 for 1 h. Cells were washed twice with PBS to remove nonadherent bacteria.

For adherence assays, wells of infected cells were incubated with 500 µL of 0.1% (v/v) Triton X-100 in sterile water for 15 min at 37 °C and the solution of lysed cells was serially diluted 10-fold and the CFU of bacteria was determined by plating on TSA for 3–5 days at 37 °C.

For invasion assays, the infected cells were washed twice with PBS and cultured in a medium containing gentamicin (100 µg / mL) to remove extracellular bacteria, and incubated at 37 °C with 5% CO_2 for 1 h. Cells were washed twice with PBS to remove gentamicin. CFU were counted to the invading bacteria.

For intracellular survival assays, after killing extracellular bacteria, the cells were incubated with DMEM containing gentamicin (20 µg / mL) and 1% FBS after being washed twice with PBS. Infected cells were washed thrice with PBS and lysed with 500 µL of 0.1% (v/v) Triton X-100 in sterile water for 15 min at 1, 4, 24, 48, and 72 h post-infection (h.p.i.). The solution of lysed cells was serially diluted 10-fold and the CFU of bacteria that survived in cells was determined by plating on TSA for 3–5 days at 37 °C. All samples were analyzed in triplicate.

Statistical analysis

Data were analyzed using GraphPad Prism 10.0 software (Graph Pad Software, San Diego, CA). Statistical significance was determined using the student's t-test. One-way or two-way analysis of variance (ANOVA) followed by Dunnett's multiple comparisons test was used for group analysis. A probability (p) value of < 0.05 was considered statistically significant.

Results

Transcriptome analysis of *B. abortus* S2308 under low Mg^{2+} conditions

Mg^{2+} is an essential micronutrient for optimal growth in vitro. To evaluate the effects of Mg^{2+} on the growth of *B. abortus* S2308, the growth curve of wild-type strain in a medium supplemented with 10 mM Mg^{2+} or in a medium with 10 µM Mg^{2+} were plotted by measuring the OD_{600}. Under the 10 µM Mg^{2+} medium, *B. abortus* S2308 survived well, but it exhibited a slow rate of growth compared to 10 mM Mg^{2+} medium at the same time points (Fig. 1A).

To explore how Mg^{2+} concentrations regulated gene expression profiles of *B. abortus*, a comparative RNA-seq analysis of *B. abortus* S2308 under high or low Mg^{2+} conditions was conducted. The total RNA was extracted from *B. abortus* S2308 under high or low Mg^{2+} conditions at the mid-phase of cell growth ($OD_{600} = 0.6$), and then the transcriptomes were sequenced to characterize differentially expressed genes (DEGs). The transcript data have been uploaded to the NCBI Sequence Read Archive (SRA) database (https://www.ncbi.nlm.nih.gov/sra), and the accession number is PRJNA1244925. A total of 3215 genes (99.6% of total genes in the *B. abortus* S2308 genome) were identified in this RNA-seq study, 262 DEGs (fold-change > 1.5 and $p < 0.05$) were found under low Mg^{2+} conditions (Supplementary File 2). Of these DEGs, 123 genes were significantly upregulated, 139 genes were significantly downregulated. According to the sequencing results, the hierarchical clustering heatmap (Fig. 1B) and the volcano plot (Fig. 1C) were plotted, displaying the significantly upregulated and downregulated DEGs in the pairwise comparisons.

GO enrichment–based cluster analysis was performed on DEGs, showing that most of them were related to the biological processes, cellular components and molecular function, such as metabolic process, cellular anatomical entity, binding, and catalytic activity (Fig. 1D). KEGG

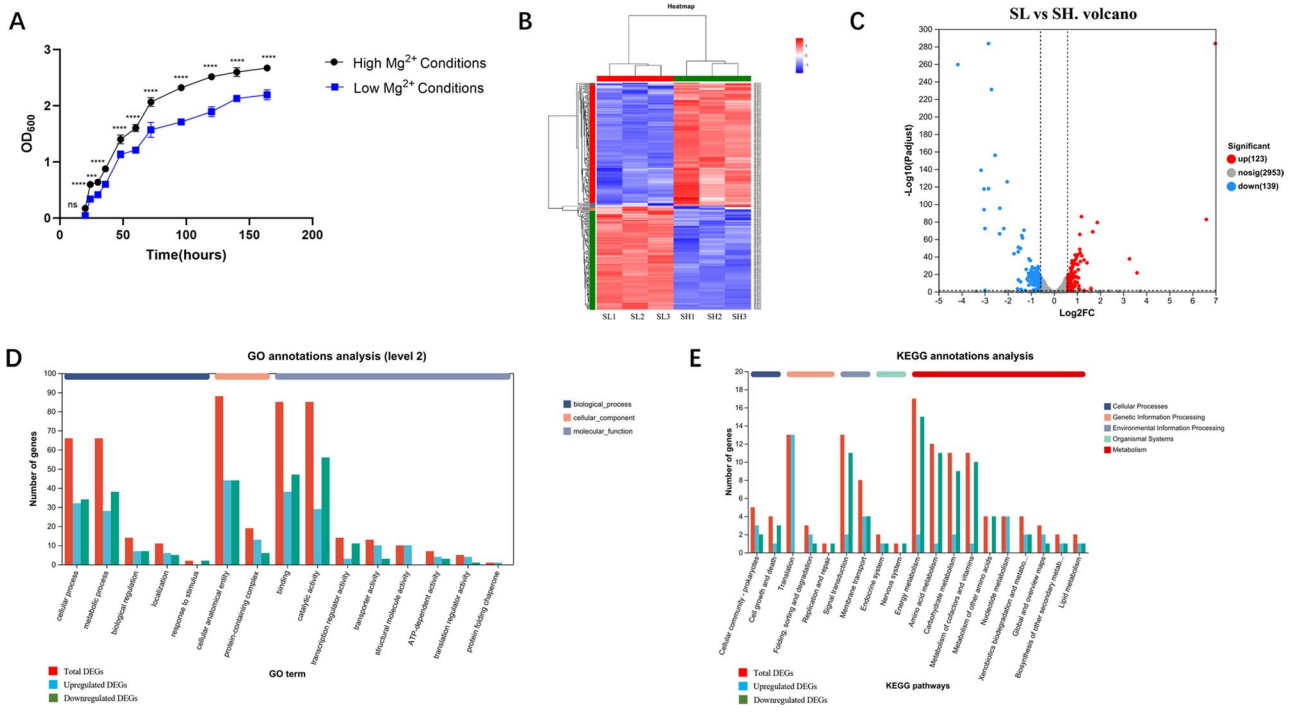

Fig. 1 Transcriptome analysis of *B. abortus* S2308 under low Mg^{2+} conditions. *B. abortus* 2308 cultured under high (10 μM) or low (10 mM) Mg^{2+} minimal medium M9 supplemented with 0.1% casamino acids, 1% yeast extract and 1% arabinose at the mid-phase of cell growth (OD_{600} = 0.6), Total RNA was extracted from bacteria and the expression of differentially expressed genes (DEGs) in *B. abortus* S2308 under high or low Mg^{2+} conditions were identified by RNA-seq. (**A**) The growth curve of *B. abortus* S2308 in high or low Mg^{2+} conditions. All the results are representative of three repeated experiments. Data were shown as the mean ± SD. The statistical significance of differences among groups was analyzed by two-way multivariate ANOVA with Tukey's post hoc test: ns, no significance. ***: $p < 0.001$, and ****: $p < 0.0001$. (**B**) Heatmap and hierarchical clusters analysis of DEGs in different comparison groups, low Mg^{2+} conditions (abbreviated to "SL") vs. high Mg^{2+} conditions (abbreviated to "SH"). Each small box indicates the expression status of a certain gene in one sample, red for up-regulated and blue for down-regulated expression. (**C**) Volcano map of DEGs in different comparison groups. The genes are colored if they pass the thresholds for P value < 0.05 and fold change ≥ 1.5, red for up-regulated and blue for down-regulated. (**D**) GO enrichment–based cluster analysis of DEGs in different comparison groups, S2308_Low_MG vs. S2308_High_MG (mRNA: red column. up-mRNA: pale blue column. down-mRNA: green column) (**E**) KEGG enrichment–based cluster analysis of DEGs in different comparison groups, S2308_Low_MG vs. S2308_High_MG (mRNA: red column. up-mRNA: pale blue column. down-mRNA: green column)

enrichment–based cluster analysis showed that the DEGs were associated with metabolism, genetic information processing, and environmental information processing, such as energy metabolism, signal transduction, and translation (Fig. 1E).

Five consecutive genes identified from RNA-seq analysis were upregulated in *B. abortus* S2308 under low Mg^{2+} conditions

Based on transcriptome analysis results, five consecutive genes in the *B. abortus* genome, BAB_RS26535 (encoding putative protein, abbreviated as HP1), BAB_RS26540 (encoding magnesium-translocating P-type ATPase, abbreviated as MgtA), BAB_RS26545 (encoding putative protein, abbreviated as HP2), BAB_RS26550 (encoding putative protein, abbreviated as HP3), and BAB_RS26555 (encoding MgtC/SapB family protein, abbreviated as MgtC), were significantly upregulated under low Mg^{2+} conditions (Fig. 2A). To confirm the authenticity of RNA-seq results, transcriptional levels of the five consecutive genes were measured in *B. abortus* S2308 under high or low Mg^{2+} conditions by RT-PCR. The results of RT-PCR for the five consecutive genes were all upregulated (Fig. 2B), consistent with the RNA-seq results.

To determine the role of five consecutive genes in the adaptation of low Mg^{2+} conditions, an in-frame deletion strain of *B. abortus* S2308 five consecutive genes (from BAB_RS26535 to BAB_RS26555), named as S2308Δ*HP1-MgtC*, and its complemented strain S2308Δ*HP1-MgtC*(pBBR1MCS-*HP1-mgtC*) were constructed respectively, and the growth curve of the mutant and its complemented strain under high or low Mg^{2+} conditions was plotted. The results showed that under the high Mg^{2+} conditions, there is no significant difference among the growth of S2308, S2308Δ*HP1-MgtC* and S2308Δ*HP1-MgtC*(pBBR1MCS-*HP1-mgtC*) (Fig. 2C). However, under the low Mg^{2+} conditions, S2308Δ*HP1-MgtC* exhibited a slow rate of growth compared to wild-type strain S2308 (Fig. 2D), and the growth curve of

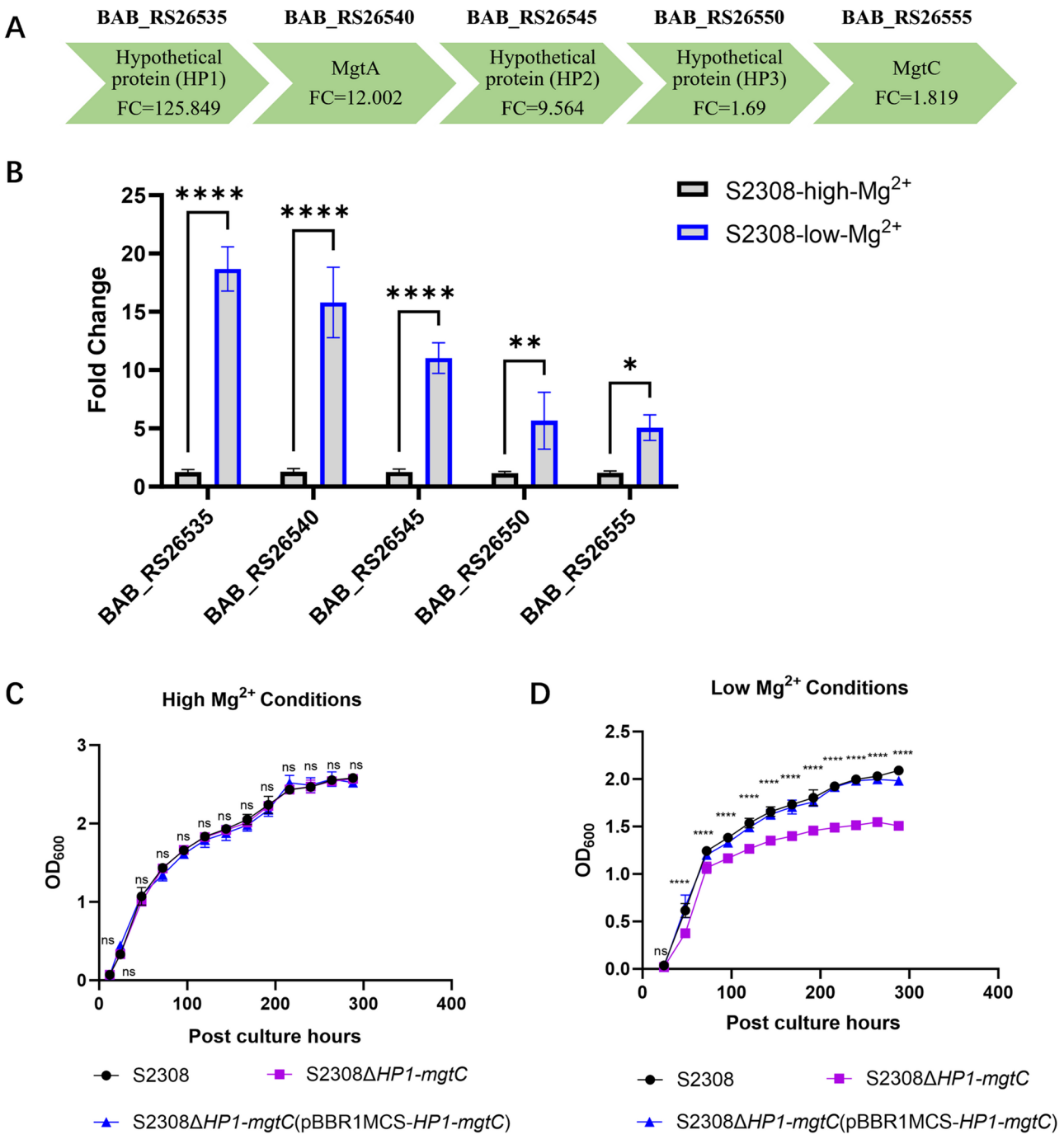

Fig. 2 Five consecutive genes identified from transcriptome analysis were upregulated in *B. abortus* S2308 under low Mg^{2+} conditions. (**A**) Schematic diagram of five consecutive DEGs and its fold change (FC) values obtained from RNAseq in *B. abortus* S2308 under high (10 μM) or low (10 mM) Mg^{2+} conditions. (**B**) qPCR verification of five consecutive DEGs in *B. abortus* S2308 under high or low Mg^{2+} conditions. (**C**&**D**) Growth curves of *B. abortus* S2308 (WT), S2308Δ*HP1-MgtC* (in-frame deletion strain of five consecutive genes) and its complemented strain S2308Δ*HP1-MgtC*(pBBR1MCS-*HP1-MgtC*) under high or low Mg^{2+} conditions. All the results are representative of three repeated experiments. Data were shown as the mean ± SD. The statistical significance of differences among groups was analyzed by one-way or two-way multivariate ANOVA with Tukey's post hoc test: ns, no significance. *: $p < 0.05$. **: $p < 0.01$. and ****:$p<0.0001$. Only the statistical significance of differences between the wild-type strain and its mutant strain were shown in the figure, and there is no significance between the wild-type strain and the complemented strain

S2308Δ*HP1-MgtC*(pBBR1MCS-*HP1-mgtC*) is similar to the wild-type strain S2308 (Fig. 2D).

HP3 and MgtC play a critical role in the adaptation of *B. abortus* to low Mg^{2+} stress responses

To determine whether HP1, MgtA, HP2, HP3 or MgtC of *B. abortus* is necessary for the growth of bacteria under Mg^{2+} starvation, we constructed the in-frame deletion of gene *HP1*, *MgtA*, *HP2*, *HP3* or *MgtC* in *B. abortus* to avoid any polar effect on downstream genes and complemented the mutation with a very low-copy plasmid. The following *B. abortus* mutant strains were constructed: S2308Δ*HP1*, S2308Δ*MgtA*, S2308Δ*HP2*, S2308Δ*HP3*, S2308Δ*MgtC*, S2308Δ*HP1*(pBBR1MCS-*HP1*), S2308Δ*MgtA*(pBBR1MCS-*MgtA*), S2308Δ*HP2*(pBBR1MCS-*HP2*), S2308Δ*HP3*(pBBR1MCS-*HP3*), S2308Δ*MgtC* (pBBR1MCS-*MgtC*), respectively. Subsequently, the growth curves of the mutant and its complemented strain under high or low Mg^{2+} conditions were plotted. Under the high Mg^{2+} conditions, the growth of mutant S2308Δ*HP1*, S2308Δ*MgtA*, S2308Δ*HP2*, S2308Δ*HP3* or S2308Δ*MgtC* is similar to the wild-type strain S2308 (Fig. 3A-E). Under the low Mg^{2+} conditions, the growth of mutant S2308Δ*HP1*, S2308Δ*MgtA*, S2308Δ*HP2* is similar to the wild-type strain S2308 (Fig. 3F-H), and S2308Δ*HP3* or S2308Δ*MgtC* exhibited a slow rate of growth compared to the wild-type strain S2308 (Fig. 3I and J).

HP3 deletion affects ATP concentrations of *B. abortus* S2308 under low Mg^{2+} conditions

Mg^{2+} represents a powerful signal arising from interconversions of adenylates (ATP, ADP and AMP) [8, 25]. In this study, we found that HP3 and MgtC were associated with the adaptation of low Mg^{2+} environment in *B. abortus* S2308. Lavigne et al. have reported that MgtC was associated with *Brucella suis* growth in a Mg^{2+}-restricted medium [21], and we have recently reported that *B. abortus* S2308 employed MgtC to maintain its metabolism through supporting the ATP hydrolysis in low Mg^{2+} environment [26]. Next, the connection between interconversions of adenylates and HP3 was detected in *B. abortus* S2308. To determine the HP3 function in bacteria ATP hydrolysis, ATP amounts of S2308, S2308Δ*HP3* and S2308Δ*HP3*(pBBR1MCS-*HP3*) under high or low Mg^{2+} conditions were conducted. The results showed that under high Mg^{2+} conditions, there was no significant difference in ATP amounts among S2308, S2308Δ*HP3* and S2308Δ*HP3*(pBBR1MCS-*HP3*) (Fig. 4), and under low Mg^{2+} conditions, the ATP amounts of S2308Δ*HP3* were significantly increased compared to S2308 and S2308Δ*HP3*(pBBR1MCS-*HP3*) (Fig. 4), highlighting that HP3 deletion affects ATP concentrations of *B. abortus* S2308 under low Mg^{2+} conditions.

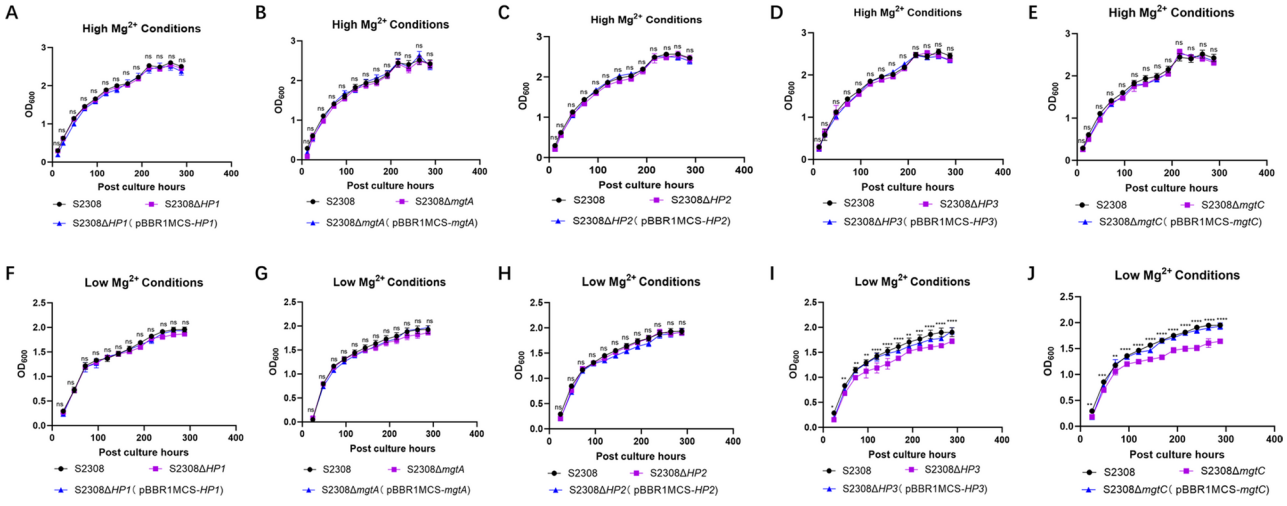

Fig. 3 HP3 and MgtC play a critical role for the adaptation of *B. abortus* to low Mg^{2+} stress responses. *B. abortus* 2308 and its derivatives were cultured under high (10 μM, up panel) or low (10 mM, down panel) Mg^{2+} conditions. Growth curves of *B. abortus* 2308 and its derivatives were plotted. (**A**) and (**F**) Growth curves of *B. abortus* S2308, S2308Δ*HP1* and its complemented strain S2308Δ*HP1* (pBBR1MCS-*HP1*). (**B**) and (**G**) Growth curves of *B. abortus* S2308, S2308Δ*MgtA* and its complemented strain S2308Δ*MgtA*(pBBR1MCS-*MgtA*). (**C**) and (**H**) Growth curves of *B. abortus* S2308, S2308Δ*HP2* and its complemented strain S2308Δ*HP2* (pBBR1MCS-*HP2*). (**D**) and (**I**) Growth curves of *B. abortus* S2308, S2308Δ*HP3* and its complemented strain S2308Δ*HP3*(pBBR1MCS-*HP3*). (**E**) and (**J**) Growth curves of *B. abortus* S2308, S2308Δ*MgtC* and its complemented strain S2308Δ*MgtC*(pBBR1MCS-*MgtC*). All the results are representative of three repeated experiments. Data were shown as the mean ± SD. The statistical significance of differences among groups was analyzed by one-way or two-way multivariate ANOVA with Tukey's post hoc test: ns, no significance. *: $p < 0.05$. **: $p < 0.01$. ***: $p < 0.001$. and ****:$p<0.0001$. Only the statistical significance of differences between the wild-type strain and its mutant strain were shown in the figure, and there is no significance between the wild-type strain and the complemented strain

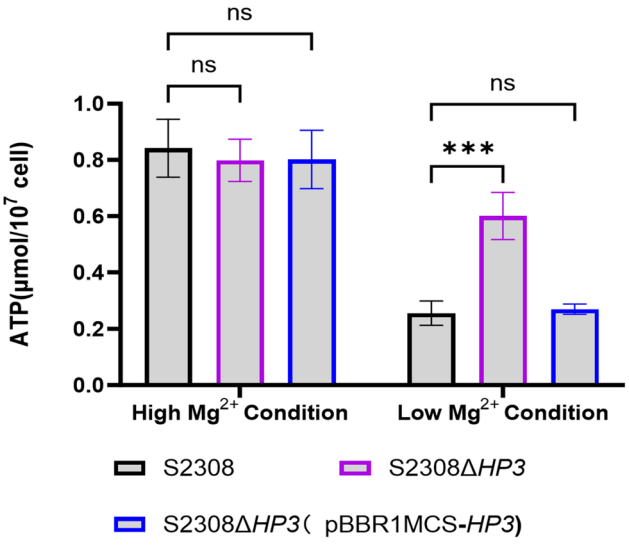

Fig. 4 HP3 deletion affects ATP concentrations of *B. abortus* S2308 under low Mg^{2+} conditions. ATP concentrations in *B. abortus* S2308, S2308Δ*HP3* and its complemented strain S2308Δ*HP3*(pBBR1MCS-*HP3*) were detected under high (10 μM) or low (10 mM) Mg^{2+} conditions. ns: no significant difference. All the results are representative of three repeated experiments. Data were shown as the mean ± SD. The statistical significance of differences among groups was analyzed by one-way or two-way multivariate ANOVA with Tukey's post hoc test: ns, no significance. ***: $p < 0.001$

S2308Δ*HP3* reduced the biofilm formation and its ability to resist polymyxin B, but not hydrogen peroxide, acidic pH, sodium Nitroprusside (SNP), ferric ion (Fe^{2+}), and osmolarity (NaCl)

To assess the ability of S2308Δ*HP3* to resist bactericidal factors, 2.5mM or 5mM hydrogen peroxide medium, 200 μg/mL or 500 μg/mL polymyxin B medium, an acidic medium, Fe^{2+} medium, NaCl medium, and SNP medium were used to evaluate its sensitivity compared to that of S2308. The results showed that compared to the wild type strain S2308, the mutant S2308Δ*HP3* exhibited similar sensitivity to the hydrogen peroxide (Fig. 5A), acidic pH (Fig. 5C), Fe^{2+} (Fig. 5D), osmolarity (NaCl) (Fig. 5E), and SNP (Fig. 5E), suggesting that HP3 did not affect *Brucella*'s ability to resist killing by oxidative stress, acidic stress, Fe^{2+} stress, osmolarity stress, and nitrosative stress. However, compared to wild type strain S2308, the mutant S2308Δ*HP3* had a significantly reduced survival rate under the medium supplemented with 200 μg/mL or 500 μg/mL polymyxin B, suggesting that HP3 affects *Brucella*'s capacity to tolerate cationic bactericidal peptides (Fig. 5B). One of the most successful strategies of microbes against environmental fluctuations might be their ability to form biofilms [27]. The biofilm-forming capacity of the mutant S2308Δ*HP3* was examined via crystal violet assay, showing that the mutant S2308Δ*HP3* exhibited a decreased biofilm-forming capacity compared to the wild type strain S2308, and the decreased biofilm-forming capacity in the S2308Δ*HP3* was completely restored by HP3 complementation (Fig. 5F).

HP3 did not affect *B. abortus* S2308 adherence, invasion and survival in RAW264.7 cells

In this study, the ability of S2308, S2308ΔHP3 and S2308ΔHP3(pBBR1MCS-HP3) to adhere to and invade RAW264.7 cells was evaluated. The adherence and invasion of the S2308ΔHP3 to RAW264.7 cells was comparable to that of S2308 (Fig. 6A). *B. abortus* is a intracellular bacterium and its virulence relies mainly on its ability to invade and replicate within professional and non-professional phagocytes [22]. To evaluated the function of HP3 in *B. abortus* virulence, the survival ability of S2308, S2308Δ*HP3* and S2308Δ*HP3*(pBBR1MCS-*HP3*) in RAW264.7 cells was evaluated at 1, 4, 24, 48, and 72 h after infection. No statistical differences in intracellular survival among S2308, S2308Δ*HP3* and S2308Δ*HP3*(pBBR1MCS-*HP3*) were detected (Fig. 6B), indicating that HP3 did not affect *B. abortus* S2308 virulence in RAW264.7 cells.

Discussion

Brucella is a facultative intracellular bacterium that was characterized by persisting for long periods within the host cells and establishing a chronic infection [28]. Within the host cells, *Brucella* will experience low cytosolic Mg^{2+}. Mg^{2+} acts as a specific signaling molecule implicated in numerous intracellular functions [29]. RNA sequencing (RNA-seq) has become an indispensable tool for transcriptome-wide analysis of differential gene expression [30]. Here, we showed the adaptation of *B. abortus* to low Mg^{2+} stress by a comprehensive analysis of global changes in the transcriptome levels.

Bacteria must acquire Mg^{2+} in a coordinated manner to achieve balanced growth and avoid loss of viability [31]. In this study, we found that the growth rate of *B. abortus* S2308 significantly decreased under low Mg^{2+} conditions at the same time points (Fig. 1A), suggesting that in vitro, Mg^{2+} is essential in *B. abortus* growth and metabolism. When *Salmonella* was exposed to Mg^{2+} starvation environment, the expression of many genes directly activated upon low extra-cytoplasmic Mg^{2+} [32, 33]. Similarly, When *B. abortus* faces Mg^{2+} starvation environment, 262 DEGs (fold-change > 1.5 and $p < 0.05$), 123 significantly upregulated genes and 139 significantly downregulated genes, were found in this study (Fig. 1B and C), suggesting that some of these genes was probably associated with the *B. abortus* growth and metabolism in the low Mg^{2+} stress responses. Mg^{2+} is involved in a multitude of essential biological processes including energy production, translation, replication, transcription, protein function and stability, through its interactions with most polyphosphate compounds, such as ATP,

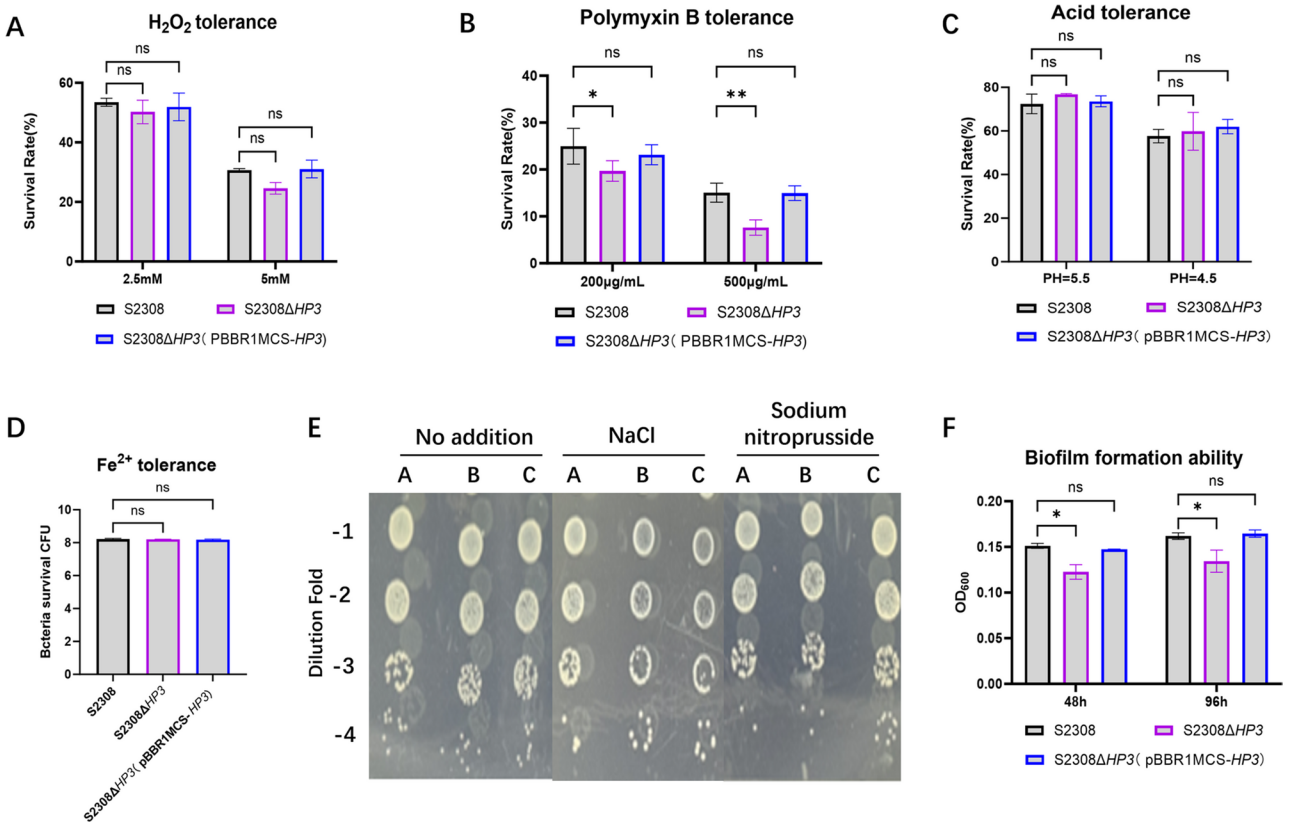

Fig. 5 Stress resistance. (**A**) Oxidative stress. The sensitivity of *B. abortus* S2308, S2308Δ*HP3* and its complemented strain S2308Δ*HP3*(pBBR1MCS-*HP3*) to 2.5mM or 5mM H_2O_2. (**B**) Cationic bactericidal peptides. The sensitivity of *B. abortus* S2308, S2308Δ*HP3* and its complemented strain S2308Δ*HP3*(pBBR1MCS-*HP3*) to 200 μg/mL or 500 μg/mL polymyxin B medium. (**C**) Acidic stress. The sensitivity of *B. abortus* S2308, S2308Δ*HP3* and its complemented strain S2308Δ*HP3*(pBBR1MCS-*HP3*) to pH = 4.5 or 5.5 acid medium. (**D**) Fe^{2+} stress. The sensitivity of *B. abortus* S2308, S2308Δ*HP3* and its complemented strain S2308Δ*HP3*(pBBR1MCS-*HP3*) to 4mM 2, 2-bipyridine (Fe^{2+} chelating agent). (**E**) Osmolarity stress and nitrosative stress. The sensitivity of *B. abortus* S2308, S2308Δ*HP3* and its complemented strain S2308Δ*HP3*(pBBR1MCS-*HP3*) to 200 mM sodium chloride (NaCl) and 0.5 mM sodium nitroprusside (SNP). "A" represents S2308; "B" represents S2308Δ*HP3*; "C" represents S2308Δ*HP3*(pBBR1MCS-*HP3*); (**F**) Biofilm formation assay was performed in *B. abortus* S2308, S2308Δ*HP3* and its complemented strain S2308Δ*HP3*(pBBR1MCS-*HP3*) using crystal violet staining. All the results are representative of three repeated experiments. Data were shown as the mean ± SD. The statistical significance of differences among groups was analyzed by one-way or two-way multivariate ANOVA with Tukey's post hoc test: ns: no significant difference. *: $P < 0.05$. **: $p < 0.01$

guanosine triphosphate (GTP), as well as other nucleotide triphosphates (NTPs), and its roles in enzyme catalysis [8, 25, 34–36]. Indeed, GO enrichment–based cluster analysis and KEGG enrichment–based cluster analysis showed that most DEGs were also associated with metabolic processes, cellular anatomical entity, binding, catalytic activity, energy metabolism, signal transduction, and translation (Fig. 1D and E), suggesting that Mg^{2+} is involved in a multitude of essential processes in *B. abortus*, which well consisted with the previous reports [7–10].

Interestingly, amongst 123 significantly upregulated DEGs identified from RNA-seq, five consecutive DEGs, *HP1*, *MgtA*, *HP2*, *HP3*, *MgtC*, were significantly upregulated in *Brucella* under Mg^{2+} starvation environment (Fig. 2). MgtA and MgtB, the members of the broad family of P-type ATPases, are responsible for transporting numerous biologically important transition metals including Ca^{2+}, Na^+/K^+, H^+/K^+, Mg^{2+}, Co^{2+}, Zn^{2+}, as well as lipids, using ATP hydrolysis to fuel transport [36, 37]. Here, we found that the in-frame deletion of gene *MgtA* did not affect the growth of *B. abortus* under the high or low Mg^{2+} conditions (Fig. 3B and G). The possible explanation is that another Mg^{2+} transporter in the *B. abortus* MgtA mutant was exploited to present the compensation function. Indeed, another Mg^{2+} transporter, *mgtE*, was significantly upregulated in *B. abortus* under Mg^{2+}-deprived environments among the DEGs identified from transcriptome analysis (Supplementary File 2). In the future studies, generating the single (*mgtE*) and double (*mgtE* and *mgtA*) mutants to provide a more comprehensive understanding of the observed phenotypes will be further conducted. MgtC, first described in *S. typhimurium*, is a virulence factor required for survival inside macrophages, full virulence in mice and growth in a low Mg^{2+} medium [38]. Consistent with the reports

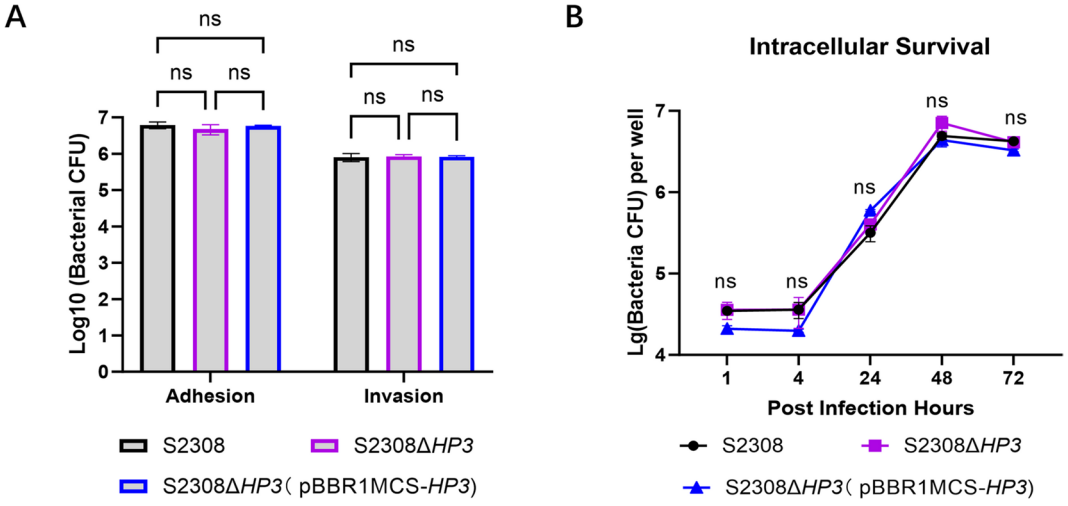

Fig. 6 HP3 did not affect *B. abortus* S2308 adherence, invasion and survival in RAW264.7 cells. Intracellular survival within RAW 264.7 macrophages. RAW264.7 cells were infected with *B. abortus* S2308, S2308Δ*HP3* and its complemented strain S2308Δ*HP3*(pBBR1MCS-*HP3*) at a MOI of 100. (**A**) Adherence and invasion detection. After incubating at 37 °C with 5% CO_2 for 1 h, adherent bacteria were enumerated. After culturing in a medium containing gentamicin (100 μg / mL) to remove extracellular bacteria, invasion bacteria were enumerated. (**B**) Cellular survival detection. The infected cells were incubated with 0.2% (v/v) Triton X-100 at 1 h, 4 h, 24 h, 48 h and 72 h p.i. Then, intracellular CFU of bacteria were enumerated. All the results are representative of three repeated experiments. Data were shown as the mean ± SD. The statistical significance of differences among groups was analyzed by one-way or two-way multivariate ANOVA with Tukey's post hoc test: ns, no significant difference

in *S. typhimurium*, *B. abortus* requires MgtC to grow in Mg^{2+}-deprived environments (Fig. 3J). Additionally, three putative proteins, HP1, HP2, HP3, were all significantly upregulated in *B. abortus* under Mg^{2+} starvation environment, and among them, only HP3 is responsible for the *B. abortus* growth in Mg^{2+}-deprived environments (Fig. 3I). However, the functions of the upregulated HP1 and HP2 need to be uncovered in future studies.

Mg^{2+} is an essential cofactor in all phosphoryl transfer reactions that involve ATP, GTP, as well as NTPs [25]. In *Salmonella*, MgtC interacts with a subunit of the F1Fo ATP synthase, hindering ATP-driven proton translocation and NADH-driven ATP synthesis in inverted vesicles leading to lower intracellular ATP levels [17]. We have recently reported that *B. abortus* employed MgtC to maintain its metabolism by supporting the ATP hydrolysis in a low Mg^{2+} environment [26], which is consistent with the results that *B. abortus* requires MgtC to grow under Mg^{2+}-deprived environments in this study. Next, our study focused on another factor HP3 which is also responsible for the *B. abortus* growth in Mg^{2+}-deprived environments. Here, the direct link between growth status and ATP levels in *B. abortus* was detected. We found that the ATP levels in the *B. abortus* HP3 deletion strain were significantly increased under low Mg^{2+} conditions (Fig. 4), demonstrating that similar to MgtC, factor HP3 was also associated with the ATP hydrolysis to maintain the growth and metabolism of *B. abortus* under low Mg^{2+} conditions. Considering that HP3 was associated with the adaptation of *B. abortus* to low Mg^{2+} stress responses, the ability of HP3 in *B. abortus* to resist bactericidal factors was accessed, showing that the HP3 deletion decreased the sensitivity of *B. abortus* to bactericidal polycations, polymyxin B (Fig. 5B). Moreover, biofilm-forming capacity was also decreased in the *B. abortus* HP3 mutant (Fig. 5F). Mg^{2+} plays crucial roles in protein synthesis by maintaining the structure of ribosomes, participating in the biochemistry of translation initiation and functioning as a counterion for ATP [45]. We hypothesized that HP3 deletion maybe result in a damaged component of the cell membrane by affecting the Mg^{2+} concentration in *B. abortus*, and the damaged cell membrane changed the tolerance of *B. abortus* to polymyxin B and biofilm formation of *B. abortus*. Additionally, we found that HP3 did not affect *Brucella* ability to resist killing by oxidative stress, acidic stress, Fe^{2+} stress, osmolarity stress, and nitrosative stress.

Bioinformatics analysis showed that HP3 protein contains a transmembrane region (amino acid positions: 21–44) and a signal peptide with cleavage occurring between amino acid positions 49 and 50. The signal peptide located behind the transmembrane region is a characterization of membrane proteins. Similarly, GO annotation analysis indicated that the HP3 protein is localized to the cell membrane. We hypothesize that the HP3 protein may be involved in sensing changes of external Mg^{2+} concentrations and transmit signals into the cell, which is similar to the function of ion channels, membrane receptors, or other membrane-associated proteins.

B. abortus is an intracellular parasite, and its virulence is mainly reflected in its intracellular survival ability. After

invading cells, *B. abortus* forms *Brucella*-containing vacuole (BCV), and various virulence factors will assist BCV break through various intracellular pressure environments, such as acidic environment, nutrient deficiency environment, and low Mg^{2+} environment, to migrate to the endoplasmic reticulum for replication [3, 38]. Among these virulence factors, MgtC is a key factor for bacteria to adapt to low Mg^{2+} environment and was responsible for the survival within macrophage in *Salmonella enterica*, *Yersinia pestis*, *Yersinia pseudotuberculosis*, *Mycobacterium tuberculosis*, *Burkholderia cenocepacia*, and *Brucella suis* [14, 21, 39–42]. In this study, the factor MgtC were identified from RNA-seq and play a critical role for in the adaptation of *B. abortus* to low Mg^{2+} stress responses. However, unlike MgtC, another factor HP3 identified from RNA-seq in this study did not affect the *B. abortus* adherence, invasion and intracellular survival (Fig. 6), suggesting that HP3 does not appear to have an appreciable effect in the *B. abortus* virulence. Further, the *B. abortus* HP3 mutant is inhibited in liquid culture at 10μM Mg^{2+} environment but not during macrophage infection, suggesting that 10μM is perhaps lower than the intracellular macrophage environment.

In this study, there are some limitations that need to be further addressed in order elucidate the functions of other DEGs identified from RNA-seq in the adaptation of *B. abortus* to low Mg^{2+} stress.

Conclusions

Altogether, this is a first description of the pattern of *B. abortus* genetic expression in response to low Mg^{2+} stress, providing insights into the behavior of *B. abortus* at the genetic level. Two factors, MgtC and HP3, played a key role in supporting the adaptation of *B. abortus* to low Mg^{2+} stress and its biological functions were elucidated, providing evidence for its possible mechanisms.

Supplementary Information

The online version contains supplementary material available at https://doi.org/10.1186/s12917-025-04831-8.

Supplementary Material 1

Supplementary Material 2

Acknowledgements

We thank National Key Research and Development Program of China, Innovation Program of Chinese Academy of Agricultural Sciences, Beijing Natural Science Foundation, for providing the funds in this study.

Author contributions

Peng Li, Nan Wang and Jianxia Jiang conceived and designed the experiments; Hengtai Wang mainly performed the experiments and analyzed the data; Lang Lv, Yike Huang, Liangquan Zhu, Huai-Ming Sang and Lei Xu helped to perform some experiments; Peng Li and Hengtai Wang wrote the manuscript; Hui Jiang, Xiaowen Yang, Jianxia JiangNan Wang and Jiabo Ding revised the manuscript and coordinated the research. All authors have read and approved the manuscript.

Funding

This work was supported by funds from the National Key Research and Development Program of China (2023YFD1800703), Innovation Program of Chinese Academy of Agricultural Sciences (CAAS-CSAB-202403), the Beijing Natural Science Foundation (6244054).

Data availability

All data supporting the findings of this study are available within the paper.

Declarations

Ethical approval

The experimental protocol was approved by Experimental Ethical Committee of Institute of Animal Science, Chinese Academy of Agricultural Sciences. *B. abortus* 2308 and its derivatives were manipulated in the Biosafety Level-3 Laboratory (BSL-3) of National/WOAH Reference Laboratory for Brucellosis, FAO Reference Centre for Brucellosis, China Institute of Veterinary Drug Control, Beijing, China.

Consent for publication

Not applicable.

Competing interests

The authors declare no competing interests.

Received: 6 December 2024 / Accepted: 14 May 2025
Published online: 21 May 2025

References

1. Corbel MJ. Brucellosis: an overview. Emerg Infect Dis. 1997;3(2):213–21.
2. Boschiroli ML, Foulongne V, O'Callaghan D. Brucellosis: a worldwide zoonosis. Curr Opin Microbiol. 2001;4(1):58–64.
3. Gorvel JP, Moreno E. *Brucella* intracellular life: from invasion to intracellular replication. Vet Microbiol. 2002;90(1–4):281–97.
4. Rambow-Larsen AA, Petersen EM, Gourley CR, Splitter GA. *Brucella* regulators: self-control in a hostile environment. Trends Microbiol. 2009;17(8):371–7.
5. Iwadate Y, Golubeva YA, Slauch JM. Cation homeostasis: coordinate regulation of polyamine and magnesium levels in *Salmonella*. mBio. 2023;14(1):e0269822.
6. Cunrath O, Bumann D. Host resistance factor SLC11A1 restricts *Salmonella* growth through magnesium deprivation. Science. 2019;366(6468):995–9.
7. Jahnen-Dechent W, Ketteler M. Magnesium basics. Clin Kidney J. 2012;5(Suppl 1):i3–14.
8. Pontes MH, Yeom J, Groisman EA. Reducing ribosome biosynthesis promotes translation during low Mg(2+) stress. Mol Cell. 2016;64(3):480–92.
9. Weiss RL, Morris DR. Cations and ribosome structure. I. Effects on the 30S subunit of substituting polyamines for magnesium ion. Biochemistry. 1973;12(3):435–41.
10. Misra VK, Draper DE. On the role of magnesium ions in RNA stability. Biopolymers. 1998;48(2–3):113–35.
11. Lee SY, Lim CJ, Droge P, Yan J. Regulation of bacterial DNA packaging in early stationary phase by competitive DNA binding of Dps and IHF. Sci Rep. 2015;5:18146.
12. Verma SC, Qian Z, Adhya SL. Architecture of the *Escherichia coli* nucleoid. PLoS Genet. 2019;15(12):e1008456.
13. Groisman EA, Kayser J, Soncini FC. Regulation of polymyxin resistance and adaptation to low-Mg^{2+} environments. J Bacteriol. 1997;179(22):7040–5.
14. Garcia Vescovi E, Soncini FC, Groisman EA. Mg^{2+} as an extracellular signal: environmental regulation of *Salmonella* virulence. Cell. 1996;84(1):165–74.
15. Snavely MD, Gravina SA, Cheung TT, Miller CG, Maguire ME. Magnesium transport in *Salmonella typhimurium*. Regulation of *MgtA* and *MgtB* expression. J Biol Chem. 1991;266(2):824–9.
16. Dalebroux ZD, Miller SI. *Salmonellae* PhoPQ regulation of the outer membrane to resist innate immunity. Curr Opin Microbiol. 2014;17:106–13.
17. Lee EJ, Pontes MH, Groisman EA. A bacterial virulence protein promotes pathogenicity by inhibiting the bacterium's own F1Fo ATP synthase. Cell. 2013;154(1):146–56.
18. Roop RM 2. Metal acquisition and virulence in Brucella. Anim Health Res Rev. 2012;13(1):10–20.

19. Evenson MA, Gerhardt P. Nutrition of *Brucellae*: utilization of iron, magnesium, and manganese for growth. Proc Soc Exp Biol Med. 1955;89(4):678–80.
20. Lestrate P, Delrue RM, Danese I, Didembourg C, Taminiau B, Mertens P, De Bolle X, Tibor A, Tang CM, Letesson JJ. Identification and characterization of *in vivo* attenuated mutants of *Brucella melitensis*. Mol Microbiol. 2000;38(3):543–51.
21. Lavigne JP, O'Callaghan D, Blanc-Potard AB. Requirement of MgtC for *Brucella suis* intramacrophage growth: a potential mechanism shared by *Salmonella enterica* and *Mycobacterium tuberculosis* for adaptation to a low-Mg^{2+} environment. Infect Immun. 2005;73(5):3160–3.
22. Li P, Tian M, Bao Y, Hu H, Liu J, Yin Y, Ding C, Wang S, Yu S. *Brucella* rough mutant induce macrophage death via activating IRE1alpha pathway of Endoplasmic reticulum stress by enhanced T4SS secretion. Front Cell Infect Microbiol. 2017;7:422.
23. Tian M, Lian Z, Bao Y, Bao S, Yin Y, Li P, Ding C, Wang S, Li T, Qi J, Wang X, Yu S. Identification of a novel, small, conserved hypothetical protein involved in *Brucella abortus* virulence by modifying the expression of multiple genes. Transbound Emerg Dis. 2019;66(1):349–62.
24. Kragh KN, Alhede M, Kvich L, Bjarnsholt T. Into the well-A close look at the complex structures of a microtiter biofilm and the crystal Violet assay. Biofilm. 2019;1:100006.
25. Klein DJ, Moore PB, Steitz TA. The contribution of metal ions to the structural stability of the large ribosomal subunit. RNA. 2004;10(9):1366–79.
26. Wang H, Lv L, Jiang H, Cheng Jun, Liu M, Chu Y, Xu J, Li P, Ding J. Biological function of MgtC protein in *Brucella abortus* to Low-Mg^{2+} resistant environment. J Anim Husb Veterinary Med (Chinese Journal).
27. Yin W, Wang Y, Liu L, He J, Biofilms. The microbial protective clothing in extreme environments. Int J Mol Sci. 2019; 20(14).
28. Zheng M, Lin R, Zhu J, Dong Q, Chen J, Jiang P, Zhang H, Liu J, Chen Z. Effector proteins of type IV secretion system: weapons of *Brucella* used to fight against host immunity. Curr Stem Cell Res Ther. 2024;19(2):145–53.
29. Pohland AC, Schneider D. Mg^{2+} homeostasis and transport in cyanobacteria - at the crossroads of bacterial and Chloroplast Mg^{2+} import. Biol Chem. 2019;400(10):1289–301.
30. Stark R, Grzelak M, Hadfield J. RNA sequencing: the teenage years. Nat Rev Genet. 2019;20(11):631–56.
31. Bruna RE, Kendra CG, Pontes MH. Coordination of phosphate and magnesium metabolism in Bacteria. Adv Exp Med Biol. 2022;1362:135–50.
32. Shin D, Lee EJ, Huang H, Groisman EA. A positive feedback loop promotes transcription surge that jump-starts *Salmonella* virulence circuit. Science. 2006;314(5805):1607–9.
33. Zwir I, Yeo WS, Shin D, Latifi T, Huang H, Groisman EA. Bacterial nucleoid-associated protein uncouples transcription levels from transcription timing. mBio. 2014;5(5):e01485–14.
34. Wacker WE. The biochemistry of magnesium. Ann N Y Acad Sci. 1969;162(2):717–26.
35. Maguire ME, Cowan JA. Magnesium chemistry and biochemistry. Biometals. 2002;15(3):203–10.
36. Zeinert R, Zhou F, Franco P, Zoller J, Lessen HJ, Aravind L, Langer JD, Sodt AJ, Storz G, Matthies D. Magnesium Transporter MgtA revealed as a Dimeric P-type ATPase. *bioRxiv*. 2024.
37. Dyla M, Kjaergaard M, Poulsen H, Nissen P. Structure and mechanism of P-Type ATPase ion pumps. Annu Rev Biochem. 2020;89:583–603.
38. Blanc-Potard AB, Lafay B. MgtC as a horizontally-acquired virulence factor of intracellular bacterial pathogens: evidence from molecular phylogeny and comparative genomics. J Mol Evol. 2003;57(4):479–86.
39. Buchmeier N, Blanc-Potard A, Ehrt S, Piddington D, Riley L, Groisman EA. A parallel intraphagosomal survival strategy shared by *mycobacterium tuberculosis* and *Salmonella enterica*. Mol Microbiol. 2000;35(6):1375–82.
40. Grabenstein JP, Fukuto HS, Palmer LE, Bliska JB. Characterization of phagosome trafficking and identification of PhoP-regulated genes important for survival of *Yersinia pestis* in macrophages. Infect Immun. 2006;74(7):3727–41.
41. Maloney KE, Valvano MA. The *MgtC* gene of *Burkholderia cenocepacia* is required for growth under magnesium limitation conditions and intracellular survival in macrophages. Infect Immun. 2006;74(10):5477–86.
42. Li P, Wang H, Sun W, Ding J. Impact of MgtC on the fitness of *Yersinia pseudotuberculosis*. Pathogens. 2023; 12(12).
43. Sun J, Dong H, Peng X, Liu Y, Jiang H, Feng Y, Li Q, Zhu L, Qin Y, Ding J. Deletion of the transcriptional regulator mucr in *Brucella canis* affects stress responses and bacterial virulence. Front Vet Sci. 2021;8:650942.
44. Kovach ME, Phillips RW, Elzer PH, Roop RM 2nd, Peterson KM. pBBR1MCS: a broad-host-range cloning vector. Biotechniques. 1994;16(5):800–2.
45. Pontes MH, Sevostyanova A, Groisman EA. When too much ATP is bad for protein synthesis. J Mol Biol. 2015;427(16):2586–94.

Publisher's note